Finite Elements in Analysis and Design 203 (2022) 103720

Contents lists available at ScienceDirect

Finite Elements in Analysis & Design

journal homepage: www.elsevier.com/locate/finel

A recursive-cluster based reduced order method for numerical prediction of effective properties of heterogeneous viscoelastic materials

Qiang Fu, Yiqian He, Xinglin Guo, Haitian Yang *

State Key Lab of Structural Analysis for Industrial Equipment, Department of Engineering Mechanics, Dalian University of Technology, Dalian, 116024, PR China

ARTICLE INFO

Keywords:
Heterogeneous viscoelastic materials
Prediction of effective properties
Direct numerical simulation
Clustering decomposition
Reduced order method
Adaptive recursive computing

ABSTRACT

A novel recursive-cluster based reduced order method is presented to predict the effective properties of heterogeneous viscoelastic materials. By virtue of a piecewise series expansion based variable separation, a temporally and spatially homogenization process is decoupled into a series of recursive elastic homogenization ones, which require only one-time clustering decomposition with one-time elastic heterogeneous analysis. Such that, the heavy computational burden caused by the direct numerical simulation over the whole domain of viscoelastic heterogeneous RUC can significantly be alleviated. The effective creep compliance or relaxation modulus is presented via a time varying average strain or average stress, and a piecewise adaptive technique is proposed to secure the temporal accuracy when step size varies. Numerical examples are provided to demonstrate the effectiveness and efficiency of proposed approach, and the predicted results agree well with those given by FEM/SBFEM based viscoelastic DNS.

1. Introduction

The determination of the effective behavior of heterogeneous viscoelastic materials from the properties of the components and the microstructure constitutes one of the major tasks in modeling their mechanical behavior and designing new materials [1]. A number of approaches have been developed to fulfill this task either in the frequency domain or in the time-domain.

Utilizing the correspondence principle [2], a viscoelastic problem is transformed into a symbolic static elastic problem in the frequency domain (transformed domain), and the effective viscoelastic properties are evaluated via an homogenization for the symbolic elastic problem and an inverse integral transformation from the frequency domain to time domain. A variety of well developed skills for the elastic homogenization provide a great convenience for the implementation of this kind of method. However, due to the difficulty of analytical inverse integral transformation, this method may suffer from the inconvenience mainly caused by the accuracy, stability, as well as computational expense of the numerical algorithms available for inversion [3–6].

The viscoelastic homogenization can also be carried out directly in the time domain, and usually needs a step by step numerical computing process using finite difference or numerical integration methods [7–11]. The inaccuracy of effective evaluation may occur because of the lower truncation order of finite difference or numerical integration methods, as well as improper step sizes which are usually difficult to predict in advance [12].

The evaluation of viscoelastic effective properties, either based upon frequency or time domains, can be conducted using various kinds of means of homogenization, such as analytical micromechanical methods and asymptotic techniques, etc.

Analytical micromechanical methods, such as Eshelby's theory [13], self-consistent scheme [14], generalized self-consistent method [15] and Mori–Tanaka method [16,17], provide effective means for the homogenization conducted in both the frequency [5,6,18–26] and time domains [12,27,28]. They can take into account statistical nature of microstructures in some extent, but are only applicable for simple microstructures and small volume fraction, and have severe limitation as nonlinear effective properties are required [29].

The asymptotic homogenization method is based on the rigorous mathematical perturbation theory with the periodicity assumption [30,31], which has been employed to characterize effective viscoelastic properties both in the frequency [32–35] and time domains [36–41].

With the rapid development of modern computer technology, the representative unit cell (RUC) [42] based direct numerical simulation (DNS) is being utilized to characterize effective properties of heterogeneous viscoelastic materials. Finite element method (FEM) [8], extended finite element method (XFEM) [43], Voronoi cell finite element method [44], quadtree scaled boundary finite element method (SBFEM) [45], etc. are used in DNS over the RUC subjected to the specified boundary conditions, the effective properties of materials are obtained by certain averaging process performed over the RUC.

* Corresponding author.
E-mail address: haitian@dlut.edu.cn (H. Yang).

https://doi.org/10.1016/j.finel.2021.103720
Received 1 August 2021; Received in revised form 25 November 2021; Accepted 30 December 2021
Available online 24 January 2022

In order to gain a reliable effective evaluation of heterogeneous viscoelastic materials and to develop the data base for further material design, DNS with a large number of samples with randomness has to be conducted via step-by-step temporal analysis in the time domain or numerical integral inversion in the frequency domain, and has to bear a heavy computational burden, thus efficient reduced order methods are in great demands.

Actually, as illustrated by [29,46], there existed various reduced order methods available for large scale complex heterogeneous problems, such as the transformation field analysis (TFA) [47], the non-uniform transformation field analysis (NTFA) [48,49], the principal component analysis [50–52] or proper orthogonal decomposition (POD) [53–55], and the proper generalized decomposition (PGD) [56–61]. These methods provide various means served for more efficient DNS based effective evaluation of heterogeneous materials. Recently, [46] proposed a novel effective model reduction method via the self-consistent clustering analysis (SCA) [46], which is based on a clustering algorithm and the Lippmann–Schwinger integral equation. By introducing and extending the cluster concept, [29] presents a FEM-Cluster Analysis based reduced order method (FCA), which can be well formulated under the framework of cluster-based minimum complementary energy [62], and is efficient for the numerical prediction of effective properties of heterogeneous material in nonlinear range, including porous materials [63]. Recently, [64] further propose a new homogenization algorithm, virtual clustering analysis (VCA), as well as provide a mathematical framework for the SCA. All these methods enable efficient predictions of nonlinear material response, such as plasticity, damage [55], and open a possible way to reduce computational expense on the DNS based effective evaluation of heterogeneous materials with time dependent constitutive relationships.

This paper follows the line of cluster decomposition based effective evaluation, and attempts to develop a new reduced order method to predict effective properties of heterogeneous viscoelastic materials in the time domain. To this end, a piecewise variable separation technique is developed via a series expansion at a discretized time interval, and is utilized to formulate a recursive elastic homogenization process without the self-consist procedure, which requires only one-time clustering decomposition with one-time elastic heterogeneous analysis. Such that, the heavy computational burden caused by the direct numerical simulation over the whole domain of viscoelastic heterogeneous RUC can significantly be alleviated. The effective creep compliance or relaxation modulus is presented via a time varying average strain or average stress, and a piecewise adaptive technique is proposed to secure the temporal accuracy when step size varies. Numerical examples are provided to demonstrate the effectiveness and efficiency of proposed approach, and the predicted results agree well with those given by FEM/SBFEM based viscoelastic DNS.

The rest of paper is organized as follows: Section 2 defines constitutive equations for heterogeneous viscoelastic materials and derives variable separation based recursive constitutive equations; Section 3 describes cluster based recursive computing of effective stress/strain; Section 4 stresses clustering decomposition and strain/stress concentration tensor; Section 5 presents numerical examples to illustrate the effectiveness and efficiency of the proposed approach. Conclusions are given in Section 6.

2. Constitutive and recursive constitutive equations

The constitutive equation of components of the heterogeneous viscoelastic material is given in form of Eq. (1) that based on a three-parameter solid model [65], as shown in Fig. 1.

$$q_0\boldsymbol{\varepsilon}(t)+q_1\frac{d\boldsymbol{\varepsilon}(t)}{dt}=\boldsymbol{G}\cdot\left(\boldsymbol{\sigma}(t)+p_1\frac{d\boldsymbol{\sigma}(t)}{dt}\right)\quad(t>0) \tag{1}$$

$$\boldsymbol{\varepsilon}(t)=\frac{1}{E_2}\boldsymbol{G}\cdot\boldsymbol{\sigma}(t)\quad(t=0) \tag{2}$$

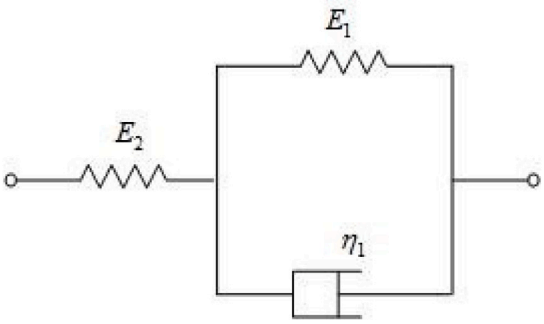

Fig. 1. Three-parameters solid model.

$$p_1=\frac{\eta}{E_1+E_2};\quad q_0=\frac{E_1E_2}{E_1+E_2};\quad q_1=\frac{E_2\eta}{E_1^I+E_2} \tag{3}$$

$$\boldsymbol{G}=\begin{bmatrix}G_{11} & G_{12} & 0\\ & G_{22} & 0\\ symm & & G_{33}\end{bmatrix} \tag{4}$$

where $\boldsymbol{\varepsilon}$ and $\boldsymbol{\sigma}$ stand for the vectors of strain and stress, respectively.

For the plane stress problem

$$G_{11}=G_{22}=1;\quad G_{12}=-\upsilon;\quad G_{33}=2(1+\upsilon) \tag{5}$$

For the plane strain problem

$$G_{11}=G_{22}=(1-\upsilon)(1+\upsilon);\quad G_{12}=-\upsilon(1+\upsilon);\quad G_{33}=2(1+\upsilon) \tag{6}$$

We divide the time domain into a number of time intervals, and the initial points and sizes of time intervals are defined by t_0, t_1, t_2,…, t_k and T_1, T_2, …, T_k, respectively.

At kth discretized time interval, $\boldsymbol{\sigma}$ and $\boldsymbol{\varepsilon}$ are expanded in term of s,

$$\boldsymbol{\sigma}=\sum_{m=0}\boldsymbol{\sigma}^m s^m \tag{7}$$

$$\boldsymbol{\varepsilon}=\sum_{m=0}\boldsymbol{\varepsilon}^m s^m \tag{8}$$

$$s=\frac{t-t_{k-1}}{T_k} \tag{9}$$

where $\boldsymbol{\sigma}^m$ and $\boldsymbol{\varepsilon}^m$ denote the vectors of expanding coefficients of $\boldsymbol{\sigma}$ and $\boldsymbol{\varepsilon}$, respectively.

At the first time interval,

$$\boldsymbol{\sigma}^0=\boldsymbol{D}\boldsymbol{\varepsilon}^0 \tag{10}$$

where $\boldsymbol{D}=E_2\cdot\boldsymbol{G}^{-1}$.

Substituting Eqs. (7)–(8) into Eq. (1) and equating the power of the two sides of equation then gives a recursive constitutive equation.

$$\boldsymbol{\sigma}^m=\boldsymbol{D}\boldsymbol{\varepsilon}^m+\boldsymbol{C}^m,\quad m=1,2,3,\ldots \tag{11}$$

where

$$\boldsymbol{C}^m=\frac{T_k}{m}\left(\frac{E_1}{\eta}\boldsymbol{D}\boldsymbol{\varepsilon}^{m-1}-\frac{1}{p_1}\boldsymbol{\sigma}^{m-1}\right) \tag{12}$$

3. Cluster based recursive computing of effective stress/strain

Assume that the RUC of interest is decomposed into M clusters according to the stress level [46], and all the elements in a cluster follow a same material law.

On the decomposed RUC, the effective stress and effective strain are defined by

$$\overline{\boldsymbol{\sigma}}=\frac{1}{V}\int_V\boldsymbol{\sigma}\mathrm{d}V=\sum_{I=1}^{M}\upsilon_I\overline{\boldsymbol{\sigma}}^I \tag{13}$$

$$\overline{\boldsymbol{\varepsilon}} = \frac{1}{V}\int_V \boldsymbol{\varepsilon} \mathrm{d}V = \sum_{I=1}^{M} v_I \overline{\boldsymbol{\varepsilon}}^I \tag{14}$$

where V stands for the volume of RUC, v_I, $\overline{\boldsymbol{\sigma}}^I$, and $\overline{\boldsymbol{\varepsilon}}^I$ denote volume fraction, effective stress, and effective strain of Ith cluster, respectively. $\overline{\boldsymbol{\sigma}}^I$ and $\overline{\boldsymbol{\varepsilon}}^I$ are defined by

$$\overline{\boldsymbol{\sigma}}^I = \frac{1}{V_I}\int_{V_I} \boldsymbol{\sigma}^I \mathrm{d}V = \sum_{m=0} \frac{1}{V_I}\int_{V_I} \boldsymbol{\sigma}^{(m,I)} \mathrm{d}V \cdot s^m = \sum_{m=0} \overline{\boldsymbol{\sigma}}^{(m,I)} s^m \tag{15}$$

$$\overline{\boldsymbol{\varepsilon}}^I = \frac{1}{V_I}\int_{V_I} \boldsymbol{\varepsilon}^I \mathrm{d}V = \sum_{m=0} \frac{1}{V_I}\int_{V_I} \boldsymbol{\varepsilon}^{(m,I)} \mathrm{d}V \cdot s^m = \sum_{m=0} \overline{\boldsymbol{\varepsilon}}^{(m,I)} s^m \tag{16}$$

where $\boldsymbol{\sigma}^{(m,I)}$ and $\boldsymbol{\varepsilon}^{(m,I)}$ stand for the mth order coefficients of $\boldsymbol{\sigma}$ and $\boldsymbol{\varepsilon}$ on the Ith cluster, $\overline{\boldsymbol{\sigma}}^{(m,I)}$ and $\overline{\boldsymbol{\varepsilon}}^{(m,I)}$ represent the mth order coefficients of $\overline{\boldsymbol{\sigma}}^I = \sum_{m=0} \overline{\boldsymbol{\sigma}}^{(m,I)} s^m$ and $\overline{\boldsymbol{\varepsilon}}^I = \sum_{m=0} \overline{\boldsymbol{\varepsilon}}^{(m,I)} s^m$, respectively.

By virtue of Eqs. (10)–(12),

$$\overline{\boldsymbol{\sigma}}^{(0,I)} = \boldsymbol{D}^I \overline{\boldsymbol{\varepsilon}}^{(0,I)} \tag{17}$$

$$\overline{\boldsymbol{\sigma}}^{(m,I)} = \boldsymbol{D}^I \overline{\boldsymbol{\varepsilon}}^{(m,I)} + \boldsymbol{C}_\alpha^{(m,I)}, \quad m = 1, 2, 3, \ldots \tag{18}$$

$$\boldsymbol{C}_\alpha^{(m,I)} = \frac{T_k}{m}\left[\frac{E_1^I}{\eta^I}\boldsymbol{D}^I \overline{\boldsymbol{\varepsilon}}^{(m-1,I)} - \frac{1}{p_1^I}\overline{\boldsymbol{\sigma}}^{(m-1,I)}\right] \tag{19}$$

Both $\overline{\boldsymbol{\sigma}}$ or $\overline{\boldsymbol{\varepsilon}}$ are expanded by

$$\overline{\boldsymbol{\sigma}} = \sum_{m=0} \overline{\boldsymbol{\sigma}}^m s^m \tag{20}$$

$$\overline{\boldsymbol{\varepsilon}} = \sum_{m=0} \overline{\boldsymbol{\varepsilon}}^m s^m \tag{21}$$

The initial values, or the zeroth order coefficients of effective strain/stress at the first time interval are given by

$$\overline{\boldsymbol{\sigma}}^0\Big|_{t=t_0} = \sum_{I=1}^{M} v_I \overline{\boldsymbol{\sigma}}^{(0,I)} = \sum_{I=1}^{M} v_I \boldsymbol{D}^I \overline{\boldsymbol{\varepsilon}}^{(0,I)} \tag{22}$$

$$\overline{\boldsymbol{\varepsilon}}^0\Big|_{t=t_0} = \sum_{I=1}^{M} v_I \overline{\boldsymbol{\varepsilon}}^{(0,I)} = \sum_{I=1}^{M} v_I (\boldsymbol{D}^I)^{-1} \overline{\boldsymbol{\sigma}}^{(0,I)} \tag{23}$$

The initial values, or the zeroth order coefficients of effective strain/stress at kth time interval are given by

$$\overline{\boldsymbol{\sigma}}^0\Big|_{t=t_k} = \sum_{m=0} \overline{\boldsymbol{\sigma}}^m\Big|_{t=t_{k-1}} \tag{24}$$

$$\overline{\boldsymbol{\varepsilon}}^0\Big|_{t=t_k} = \sum_{m=0} \overline{\boldsymbol{\varepsilon}}^m\Big|_{t=t_{k-1}} \tag{25}$$

At kth time interval, k = 1,2..., mth order coefficients of effective strain/stress are given by

$$\overline{\boldsymbol{\sigma}}^m = \sum_{I=1}^{M} v_I \overline{\boldsymbol{\sigma}}^{(m,I)} = \sum_{I=1}^{M} v_I [\boldsymbol{D}^I \overline{\boldsymbol{\varepsilon}}^{(m,I)} + \boldsymbol{C}_\alpha^{(m,I)}], \quad m = 1, 2, 3, \ldots \tag{26}$$

$$\overline{\boldsymbol{\varepsilon}}^m = \sum_{I=1}^{M} v_I \overline{\boldsymbol{\varepsilon}}^{(m,I)} = \sum_{I=1}^{M} v_I (\boldsymbol{D}^I)^{-1} [\overline{\boldsymbol{\sigma}}^{(m,I)} - \boldsymbol{C}_\alpha^{(m,I)}], \quad m = 1, 2, 3, \ldots \tag{27}$$

Assume the RUC is subjected to a uniform stress $\widetilde{\boldsymbol{\sigma}} = \sum_{m=0} \widetilde{\boldsymbol{\sigma}}^m s^m = constant$.

In light of [66],

$$\overline{\boldsymbol{\sigma}} = \widetilde{\boldsymbol{\sigma}} \tag{28}$$

and then

$$\overline{\boldsymbol{\sigma}}^0 = \widetilde{\boldsymbol{\sigma}} \tag{29}$$

$$\overline{\boldsymbol{\sigma}}^m = \widetilde{\boldsymbol{\sigma}}^m = 0, \quad m = 1, 2, 3, \ldots \tag{30}$$

Substituting Eqs. (22) and (26) into Eqs. (29)–(30) then yields

$$\sum_{I=1}^{M} v_I \boldsymbol{D}^I \overline{\boldsymbol{\varepsilon}}^{(0,I)} = \widetilde{\boldsymbol{\sigma}} = \widetilde{\boldsymbol{\sigma}}^{0*} \tag{31}$$

$$\sum_{I=1}^{M} v_I \boldsymbol{D}^I \overline{\boldsymbol{\varepsilon}}^{(m,I)} = -\sum_{I=1}^{M} v_I \boldsymbol{C}_\alpha^{(m,I)} = \widetilde{\boldsymbol{\sigma}}^{m*}, \quad m = 1, 2, 3, \ldots \tag{32}$$

Eqs. (31)–(32) mean that $\overline{\boldsymbol{\varepsilon}}^{(m,I)}$ can be evaluated via a series of homogenizations on a same elastic heterogeneous RUC, which is subjected to a series of uniform stresses $\widetilde{\boldsymbol{\sigma}}^{m*}$ (m = 0,1,2,...), and $\overline{\boldsymbol{\varepsilon}}^m$ can be determined by $\overline{\boldsymbol{\varepsilon}}^m = \sum_{I=1}^{M} v_I \overline{\boldsymbol{\varepsilon}}^{(m,I)}$, consequently, $\overline{\boldsymbol{\varepsilon}}$ can be achieved via Eq. (21).

Since the homogenizations of Eqs. (31)–(32) are conducted on a same elastic heterogeneous RUC with the same model of stress boundary condition, it is reasonable to assume

$$\overline{\boldsymbol{\sigma}}^{(m,I)} = \boldsymbol{B}^I \cdot \overline{\boldsymbol{\sigma}}^m \tag{33}$$

where $\boldsymbol{B}^I$ stand for a stress concentration matrix corresponding to a unit uniform stress.

At the first time interval,

$$\overline{\boldsymbol{\varepsilon}}^0\Big|_{t=t_0} = \sum_{I=1}^{M} v_I \overline{\boldsymbol{\varepsilon}}^{(0,I)} = \sum_{I=1}^{M} v_I (\boldsymbol{D}^I)^{-1} \overline{\boldsymbol{\sigma}}^{(0,I)} = \sum_{I=1}^{M} v_I (\boldsymbol{D}^I)^{-1} \boldsymbol{B}^I \cdot \widetilde{\boldsymbol{\sigma}}^{0*} \tag{34}$$

At the kth time interval,

$$\overline{\boldsymbol{\varepsilon}}^0\Big|_{t=t_k} = \sum_{m=0} \overline{\boldsymbol{\varepsilon}}^m\Big|_{t=t_{k-1}} \tag{35}$$

When m = 1, 2, 3, ...,

$$\overline{\boldsymbol{\varepsilon}}^m = \sum_{I=1}^{M} v_I (\boldsymbol{D}^I)^{-1} \boldsymbol{B}^I \cdot \widetilde{\boldsymbol{\sigma}}^{m*} \tag{36}$$

By calculating $\overline{\boldsymbol{\varepsilon}} = \sum_{m=0} \overline{\boldsymbol{\varepsilon}}^m s^m$ interval by interval with Eqs. (31)–(32), the effective strains of RUC are acquired, by which the creep compliance of a heterogeneous viscoelastic material can be evaluated.

To ensure temporal accuracy of $\overline{\boldsymbol{\varepsilon}}$, an adaptive computing process is designed with a convergence criteria.

$$\frac{\left\|\overline{\boldsymbol{\varepsilon}}^m\right\|}{\left\|\sum_{n=0}^{m} \overline{\boldsymbol{\varepsilon}}^n\right\|} \le \beta \tag{37}$$

where β is a prescribed error tolerance and $\|\bullet\|$ represents a L^2-norm.

In the recursive computing, the upper limit of expansion order is empirically pre-set by $m = m_{up}$. Eq. (37) is checked when each $\overline{\boldsymbol{\varepsilon}}^m$ is obtained. If it is satisfied at $m<m_{up}$, the computation at the current time interval will stop and step into the next. If it is not satisfied till $m = m_{up}$, the size of time interval will be reduced. A more refined rule concerned with upper limit and step size has been presented in the authors previous work [67,68].

When a uniform strain $\widetilde{\boldsymbol{\varepsilon}} = \sum_{m=0} \widetilde{\boldsymbol{\varepsilon}}^m s^m = constant$ is imposed on the boundary of RUC.

$$\overline{\boldsymbol{\varepsilon}} = \widetilde{\boldsymbol{\varepsilon}} \tag{38}$$

$$\overline{\boldsymbol{\varepsilon}}^0 = \widetilde{\boldsymbol{\varepsilon}} \tag{39}$$

$$\overline{\boldsymbol{\varepsilon}}^m = \widetilde{\boldsymbol{\varepsilon}}^m = 0, \quad m = 1, 2, 3, \ldots \tag{40}$$

$$\sum_{I=1}^{M} v_I (\boldsymbol{D}^I)^{-1} \overline{\boldsymbol{\sigma}}^{(0,I)} = \sum_{I=1}^{M} v_I \overline{\boldsymbol{\varepsilon}}^{(0,I)} = \widetilde{\boldsymbol{\varepsilon}} = \widetilde{\boldsymbol{\varepsilon}}^{0*} \tag{41}$$

$$\sum_{I=1}^{M} v_I (\boldsymbol{D}^I)^{-1} \overline{\boldsymbol{\sigma}}^{(m,I)} = \sum_{I=1}^{M} v_I (\boldsymbol{D}^I)^{-1} \boldsymbol{C}_\alpha^{(m,I)} = \widetilde{\boldsymbol{\varepsilon}}^{m*}, \quad m = 1, 2, 3, \ldots \tag{42}$$

Due to the similar reasons for Eq. (33), it is reasonable to assume

$$\overline{\boldsymbol{\varepsilon}}^{(m,I)} = \boldsymbol{A}^I \cdot \overline{\boldsymbol{\varepsilon}}^m \tag{43}$$

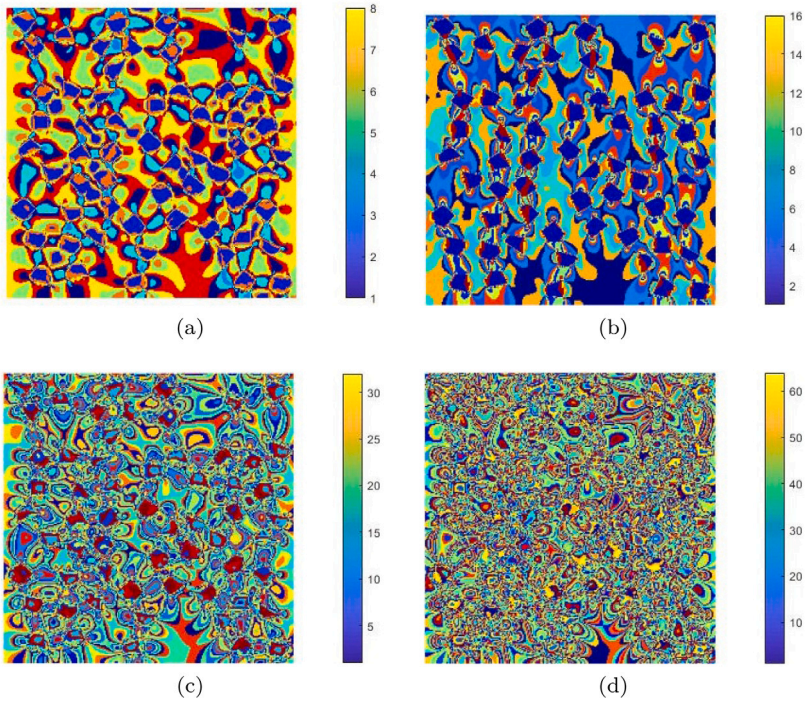

Fig. 2. Clustering decomposition: (a) 8 clusters; (b) 16 clusters; (c) 32 clusters; (d) 64 clusters. (For interpretation of the references to color in this figure legend, the reader is referred to the web version of this article.)

where A^I stand for a strain concentration matrix corresponding to a unit uniform strain.

At the first time interval,

$$\overline{\boldsymbol{\sigma}}^0\Big|_{t=t_0} = \sum_{I=1}^{M} v_I \overline{\boldsymbol{\sigma}}^{(0,I)} = \sum_{I=1}^{M} v_I \boldsymbol{D}^I \overline{\boldsymbol{\varepsilon}}^{(0,I)} = \sum_{I=1}^{M} v_I \boldsymbol{D}^I \boldsymbol{A}^I \cdot \widetilde{\boldsymbol{\varepsilon}}^{0*} \tag{44}$$

At the kth time interval,

$$\overline{\boldsymbol{\sigma}}^0\Big|_{t=t_k} = \sum_{m=0} \overline{\boldsymbol{\sigma}}^m\Big|_{t=t_{k-1}} \tag{45}$$

When $m = 1, 2, 3, \ldots,$

$$\overline{\boldsymbol{\sigma}}^m = \sum_{I=1}^{M} v_I \boldsymbol{D}^I \boldsymbol{A}^I \cdot \widetilde{\boldsymbol{\varepsilon}}^{m*} \tag{46}$$

By calculating $\overline{\boldsymbol{\sigma}} = \sum_{m=0} \overline{\boldsymbol{\sigma}}^m s^m$ interval by interval with Eqs. (41)–(42), the effective stress of RUC is acquired, by which the relaxation modules of a heterogeneous viscoelastic material can be evaluated.

An adaptive computing process similar to Eq. (37) is employed to calculate $\overline{\boldsymbol{\sigma}}$.

4. Cluster decomposition and strain/stress concentration tensor

Based upon a high fidelity FE simulation on the heterogeneous elastic RUC with D^I, the stress solution can be obtained with $\widetilde{\boldsymbol{\sigma}} = \{\widetilde{\sigma}, 0, 0\}^T$. Utilizing the k-means algorithm [69], V is decomposed into M virtual subdomains V_I, $I = 1, 2, \ldots, M$, by classifying all FE elements into M clusters according to the element stress levels in the X direction. Each cluster may consist of several geometrically disjointed sub-domains with the same D^I, as shown in Fig. 2 where one color refers to one cluster. The effective stress/strain of V_I are given by Eqs. (15)–(16).

$$V = \sum_{I=1}^{M} V_I \tag{47}$$

$$V_I \cap V_J = \emptyset, \quad I \neq J, I, J = 1, 2, \ldots, M \tag{48}$$

For $\widetilde{\boldsymbol{\sigma}} = \{\widetilde{\sigma}, 0, 0\}^T$, B^I is given by

$$\boldsymbol{B}^I = \begin{bmatrix} \overline{\sigma}_x^{(0,I)}/\widetilde{\sigma} & 0 & 0 \\ \overline{\sigma}_y^{(0,I)}/\widetilde{\sigma} & 0 & 0 \\ \overline{\tau}_{xy}^{(0,I)}/\widetilde{\sigma} & 0 & 0 \end{bmatrix} \tag{49}$$

Using $\widetilde{\boldsymbol{\sigma}} = \{\widetilde{\sigma}, 0, 0\}^T$, the $\overline{\varepsilon}_x$ and $\overline{\varepsilon}_y$ accompanied by $\overline{\varepsilon}_x$ can be obtained.

For $\widetilde{\boldsymbol{\varepsilon}} = \{\widetilde{\varepsilon}, 0, 0\}^T$, A^I is given by

$$\boldsymbol{A}^I = \begin{bmatrix} \overline{\varepsilon}_x^{(0,I)}/\widetilde{\varepsilon} & 0 & 0 \\ \overline{\varepsilon}_y^{(0,I)}/\widetilde{\varepsilon} & 0 & 0 \\ \overline{\gamma}_{xy}^{(0,I)}/\widetilde{\varepsilon} & 0 & 0 \end{bmatrix} \tag{50}$$

In this case, $\overline{\sigma}_x$ and $\overline{\sigma}_y$ accompanied by $\overline{\sigma}_x$ can be obtained.

Utilizing the time varying effective strain or effective stress above, the creep compliance or relaxation modulus can be estimated by solving an optimization problem described in Appendix.

It is worthy to note that for 2-D problem, other creep compliances or relaxation moduli can be evaluated with $\widetilde{\boldsymbol{\sigma}} = \{0, \widetilde{\sigma}, 0\}^T$ and $\widetilde{\boldsymbol{\sigma}} = \{0, 0, \widetilde{\sigma}\}^T$ or with $\widetilde{\boldsymbol{\varepsilon}} = \{0, \widetilde{\varepsilon}, 0\}^T$ and $\widetilde{\boldsymbol{\varepsilon}} = \{0, 0, \widetilde{\varepsilon}\}^T$.

5. Numerical verification

Four numerical examples are presented to verify the effectiveness of proposed approach. The first example examines the impacts of inclusion distribution and step size on the proposed method, the second one is mainly concerned with the number of clusters and computational efficiency. In the third example, the Scaled Boundary Finite Element Method (SBFEM) and an image based quadtree technique are combined in the FE analysis of elastic heterogeneous RUC, and the coefficients in effective creep compliance are estimated. The last example addresses an effective evaluation of relaxation modulus. ABAQUS based direct numerical simulations (ABAQUS-DNS) on the heterogeneous viscoelastic RUCs are conducted to provide the reference for the time varying effective strains.

For simplicity, all variables and parameters are assumed dimensionless and a uniform step size is adopted.

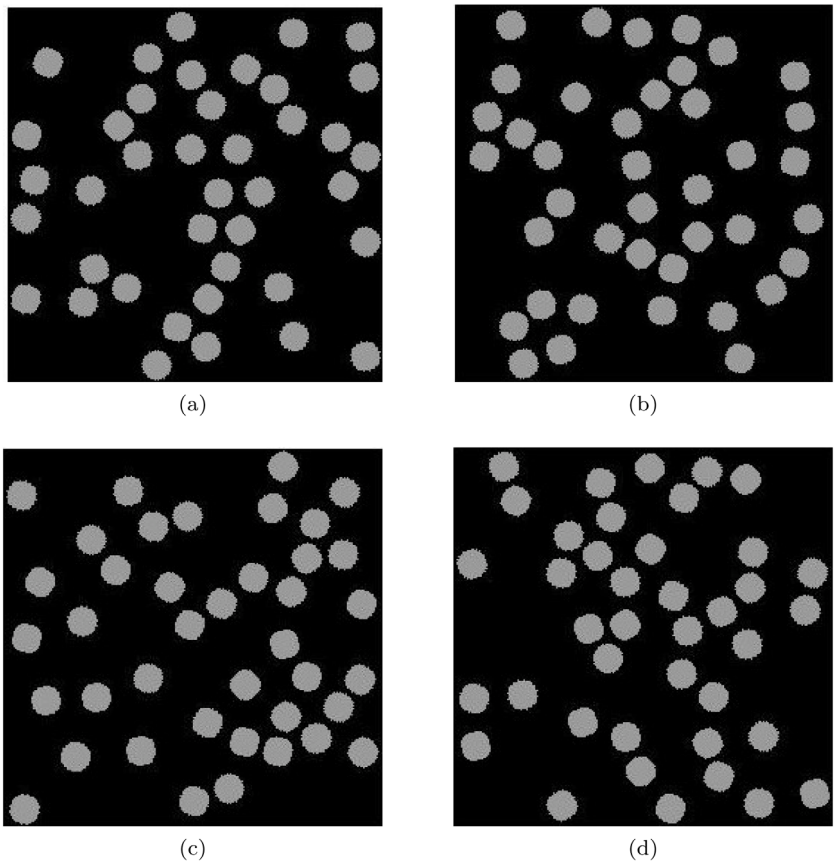

Fig. 3. RUCs with different distributions of 40 inclusions.

Table 1
Constitutive parameters.

	Matrix	Inclusion
μ	0.2	0.3
η	6000	60 000
E_1	6000	60 000
E_2	6000	60 000

5.1. Example 1

Consider a heterogeneous material composed of the viscoelastic matrix and circular inclusions, the constitutive parameters of the matrix and inclusion are given in Table 1 [22]. The volume fraction of inclusions is $v_f = 19.18\%$. Computing parameters are given by $\beta = 10^{-6}$ and $M = 8$.

An ABAQUS based converged solution is provided for the FE analysis on the heterogeneous elastic RUC (19 057 elements, 20 647 nodes).

The effective strains are obtained for four RUCs with same size but different randomly produced distributions of inclusions, as shown in Fig. 3. The mean of these four effective strains is taken as the effective strains. Table 2 exhibits comparisons of $\overline{\varepsilon}_x$ given by proposed method and ABAQUS-DNS, and the maximum relative deviation is 0.022%. Fig. 4 shows a comparison of the effective Poisson's ratio which is nearly time independent. Table 3 provides a comparison of $\overline{\varepsilon}_x$ with different step sizes. Table 4 presents a comparison of $\overline{\varepsilon}_x$ with the same volume fraction and same size of inclusions, but with different RUC sizes, as shown in Fig. 5.

5.2. Example 2

Consider the material same as Example 1, but inclusions are polygonal, as shown in Fig. 6. The volume fraction of inclusions is $v_f = 17.28\%$. Computing parameters are given by $\beta = 10^{-6}$, $\Delta t = 0.1$.

An ABAQUS based converged solution is provided for the FE analysis on the heterogeneous elastic RUC (65 a536 elements, 66 049 nodes). Fig. 7 and Table 5 present comparisons of $\overline{\varepsilon}_x$ and $\overline{\varepsilon}_y$ given by proposed method with different number of clusters and ABAQUS-DNS, and the maximum relative deviation is 0.17% (8 clusters). Tables 6 and 7 show the comparisons of computational costs spent by the proposed method and ABAQUS-DNS.

5.3. Example 3

Consider the material same as Example 1, but inclusions are elliptical with a 1/2 aspect ratio. The volume fraction of inclusions is 23.97%. Computing parameters are given by $\beta = 10^{-6}$, $\Delta t = 0.1$.

The proposed reduced order method can not only be conducted under the conventional FE framework, but also under the framework of Scale Boundary Finite Element Method. In this example, SBFEM is combined with the quadtree technique [70], providing a convenience of mesh generation by directly using the image of RUC [71], as shown in Fig. 8. The SBFEM is provided for the FE analysis on the heterogeneous elastic RUC (15 433 elements, 18 949 nodes) and the TPAA-SBFEM [45] based converged solutions are taken as the reference solutions.

Fig. 9 shows comparisons of $\overline{\varepsilon}_x$ and $\overline{\varepsilon}_y$ with different number of clusters, the maximum relative deviation is 0.186%. Table 8 shows a comparison of computational costs spent by the proposed method and TPAA-SBFEM. By solving the optimization problem defined in Appendix, the coefficients of a Prony series based effective creep compliance $\overline{J}(t)$ are estimated using time varying $\overline{\varepsilon}_x$, as shown in Table 9.

Table 2
A comparison of $\bar{\varepsilon}_x$ given by proposed method and ABAQUS-DNS.

Method	Distribution	t = 0	t = 2	t = 4	t = 6	t = 8
Proposed method	a	0.000123822	0.000231153	0.000245448	0.000247351	0.000247601
	b	0.000123901	0.000231109	0.000245552	0.000247498	0.000247756
	c	0.000125286	0.000233656	0.000248287	0.000250263	0.000250525
	d	0.000124068	0.000231371	0.000245870	0.000247829	0.000248090
	Mean	0.000124269	0.000231822	0.000246289	0.000248235	0.000248493
ABAQUS-DNS	a	0.000123822	0.000230886	0.000245376	0.000247337	0.000247598
	b	0.000123901	0.000231033	0.000245532	0.000247494	0.000247755
	c	0.000125286	0.000233615	0.000248276	0.000250260	0.000250525
	d	0.000124068	0.000231345	0.000245863	0.000247828	0.000248089
	Mean	0.000124269	0.000231720	0.000246262	0.000248230	0.000248492

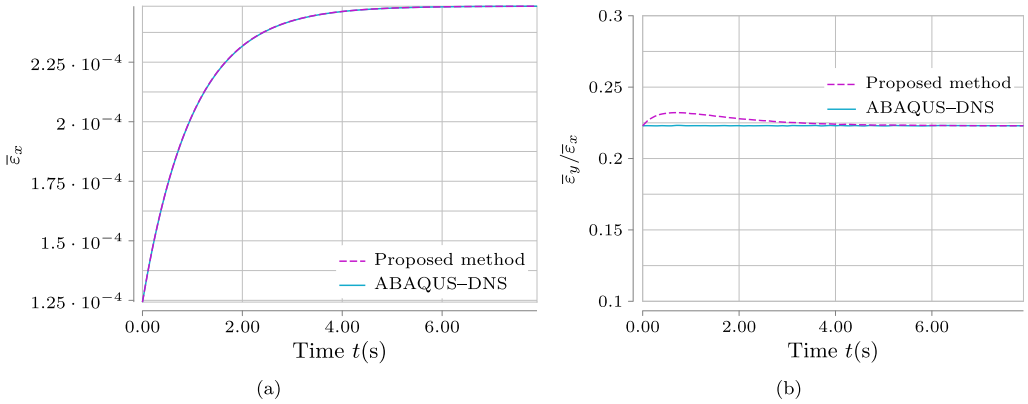

Fig. 4. Comparisons of time varying $\bar{\varepsilon}_x$ and $\bar{\varepsilon}_y/\bar{\varepsilon}_x$.

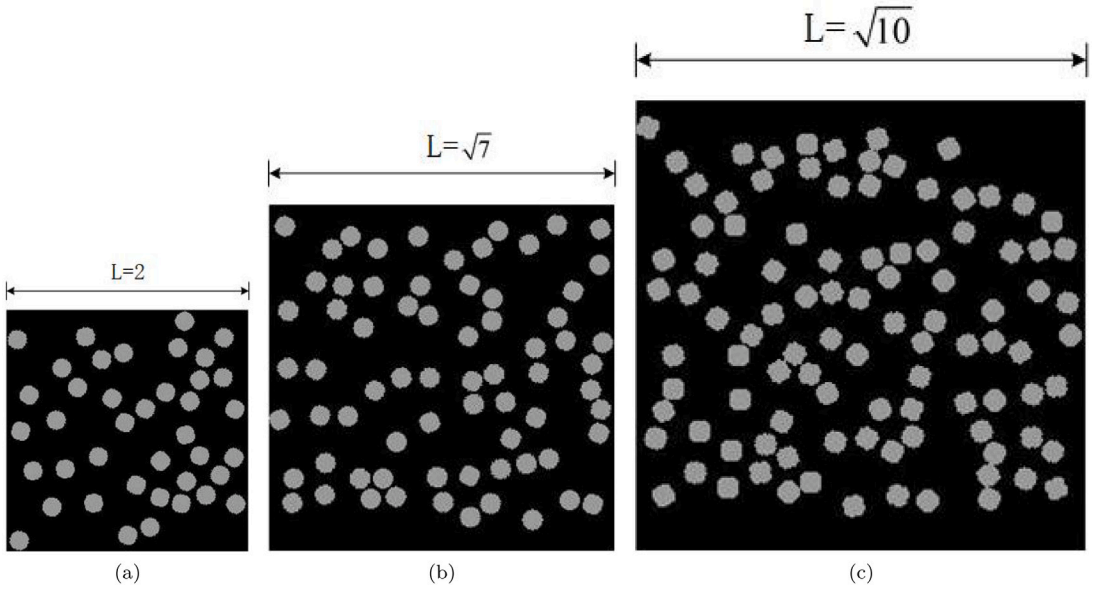

Fig. 5. RUCs with the same volume fraction but different RUC sizes: (a) 40 inclusions; (b) 70 inclusions; (c) 100 inclusions.

Table 3
A comparison of $\bar{\varepsilon}_x$ with different step sizes.

Step size	t = 0	t = 2	t = 4	t = 6	t = 8
$\Delta t = 0.1$	0.000124269	0.000231822	0.000246289	0.000248235	0.000248493
$\Delta t = 0.2$	0.000124269	0.000231822	0.000246289	0.000248235	0.000248493
$\Delta t = 0.4$	0.000124269	0.000231822	0.000246289	0.000248235	0.000248493
$\Delta t = 0.8$	0.000124269	0.000231822	0.000246289	0.000248235	0.000248493

Table 4
A comparison of $\bar{\varepsilon}_x$ with different RUC sizes.

RUC size	t = 0	t = 2	t = 4	t = 6	t = 8
$L = 2$	0.000124269	0.000231720	0.000246262	0.000248230	0.000248492
$L = \sqrt{7}$	0.000124614	0.000232582	0.000247204	0.000248982	0.000249195
$L = \sqrt{10}$	0.000124339	0.000231851	0.000246401	0.000248370	0.000248633

Table 5
A comparison of $\bar{\varepsilon}_x$ given by proposed method and ABAQUS-DNS.

Method	t = 0	t = 2	t = 4	t = 6	t = 8
8 clusters	0.000127709	0.000238390	0.000253148	0.000255116	0.000255374
16 clusters	0.000127709	0.000238202	0.000253098	0.000255106	0.000255372
32 clusters	0.000127709	0.000238121	0.000253076	0.000255101	0.000255371
64 clusters	0.000127709	0.000238099	0.000253070	0.000255100	0.000255371
ABAQUS-DNS	0.000127709	0.000238135	0.000253080	0.000255102	0.000255371

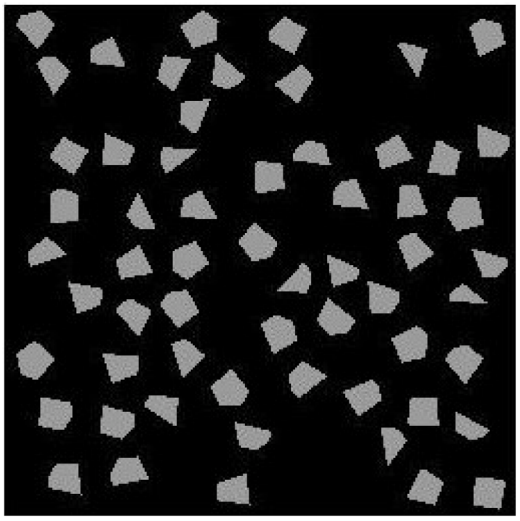

Fig. 6. A RUC with polygonal inclusions.

Table 6
A comparison of computational efficiency with respect to different step sizes.

Method	Step size	Proposed method				ABAQUS-DNS
		8 clusters	16 clusters	32 clusters	64 clusters	
CPU time	$\Delta t = 0.1$	56.0 s	57.8 s	58.9 s	61.0 s	752.4 s
	$\Delta t = 0.01$	64.0 s	64.7 s	67.5 s	69.0 s	5199.3 s

5.4. Example 4

Consider the material and internal geometry of RUC same as Example 1, but a uniform strain boundary conditions is applied. The volume fraction of circular inclusions is 30%. Computing parameters are given by $\beta = 10^{-6}$, $\Delta t = 0.1$.

An ABAQUS based converged solution is provided for the FE analysis on the heterogeneous elastic RUC (12 100 elements, 12 113 nodes). Fig. 10 shows comparisons of $\bar{\sigma}_x$ with different number of clusters, the maximum relative deviations are shown in Table 10.

5.5. Computing remarks

Numerical results indicate

1. The proposed method is applicable to predict the effective creep and relaxation behaviors via time varying average strain or average stress.
2. The effective strains evaluated by the proposed method agree well with those given by ABAQUS-DNS or TPAA-SBFEM-DNS. As shown in Tables 2 and 5 and Fig. 9, the maximum relative deviations of proposed method is only 0.186%.
3. For different step sizes, a stable temporal accuracy of effective strains can be secured by piecewise adaptive computing, as shown in Table 3.
4. Because only one-time elastic heterogeneous FE analysis is required for the proposed method, its computational cost is much cheaper than those of ABAQUS-DNS or TPAA-SBFEM, and becomes more cheaper with the decrease of step size and the increase of FE scale, as shown in Tables Tables 6–8, respectively.
5. The heterogeneous elastic analysis for the clustering decomposition on RUC can be fulfilled by various well developed numerical techniques, in addition to FE, SBFEM is employed in this paper, which takes advantages of tackling the problem with stress singularity and image based mesh generating.
6. For the DNS-clustering based effective evaluation, cluster and mesh convergence tests should be basic guarantees for the fine gradation of stress and accurate initial solutions, and are conducted in this paper.
7. For all the numerical examples, $m_{up} = 30$, and all the recursive computing is converged at $m < m_{up}$.

6. Conclusions

A novel reduced order method is presented to evaluate effective properties of heterogeneous viscoelastic materials, which is attractive as it requires no self-consist process, only one-time elastic FE analysis for clustering decomposition, and a temporally piecewise recursive adaptive computing process with very few unknowns of effective strain/stress. The major merits of presented work include:

1. A piecewise variables separation technique is developed by a series expansion at a discretized time interval, and a temporally and spatially coupled effective evaluation process is converted into a series of elastic evaluation processes, and the whole process requires only one-time elastic heterogeneous FE analysis and needs no self-consist process.
2. The proposed method is conducted in the time domain, thus all the inconvenience caused by the integral inversion in the integral transformation methods can be avoided.
3. The temporal accuracy of evaluation is secured by a recursive adaptive process, and the inaccuracy caused by the lower truncation order of FDM can be avoided.
4. In this paper, the effective strain and creep compliance are evaluated under a constant stress boundary condition, by imposing a constant strain boundary conditions, the effective stress and relaxation modulus can also be evaluated using the proposed approach.

The present formulation is applicable to the linear viscoelastic model with one order derivative of stress and strain, and can be conveniently to extend the linear viscoelastic model with higher order derivatives because a similar but more complex variable separation based recursive symbolic elastic homogenization process and an adaptive algorithm to acquire the effective strain/stress can be derived. The ROM (reduced order method) presents potential benefits and applications to the efficient optimization concerned with material designs. For instance, in designing material micro-structures by using isogeometric analysis and parameterized level set method, a reduced modeling combined with topology optimization was developed to improve the computational efficiency [72]. The major objective of presented work is to provide effective means for the effective evaluation of heterogeneous viscoelastic materials, and should be extended to the issue concerned with material design which has been taken as the focus at the next step, but needs more efforts.

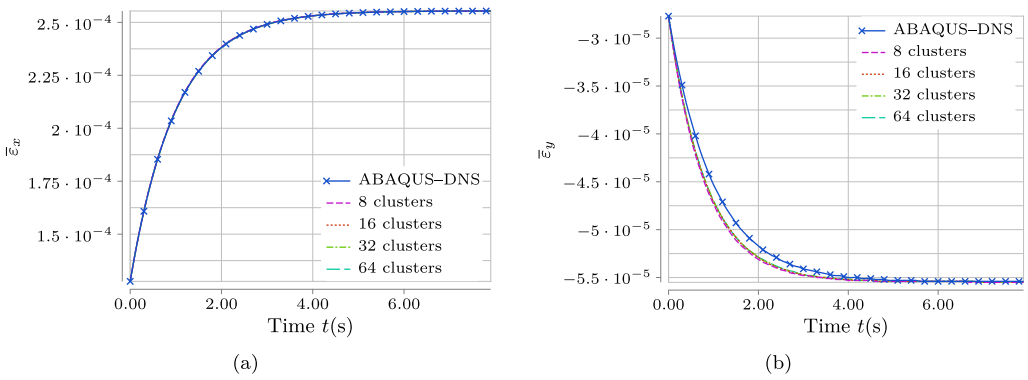

Fig. 7. Comparisons of time varying effective strains.

Table 7
A comparison of computational efficiency with respect to different FE scales.

Method	FE scale	Proposed method				ABAQUS-DNS
		8 clusters	16 clusters	32 clusters	64 clusters	
CPU time	66 049 nodes	56.0 s	57.8 s	58.9 s	61.0 s	752.4 s
	263 169 nodes	132.1 s	136.7 s	139.4 s	146.2 s	2051.6 s

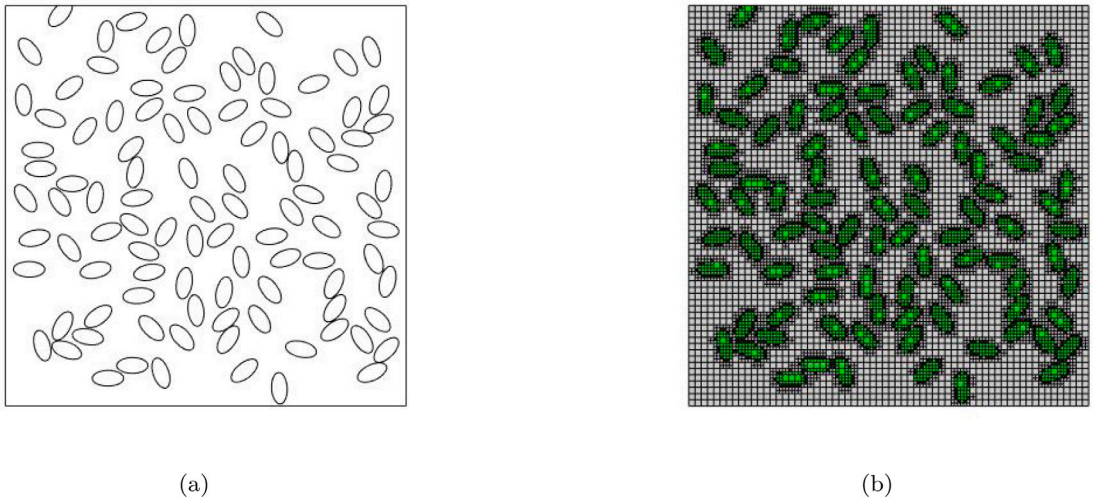

Fig. 8. A RUC with elliptical inclusions (a) and its SBFEM mesh generated by image based quadtree technique (b).

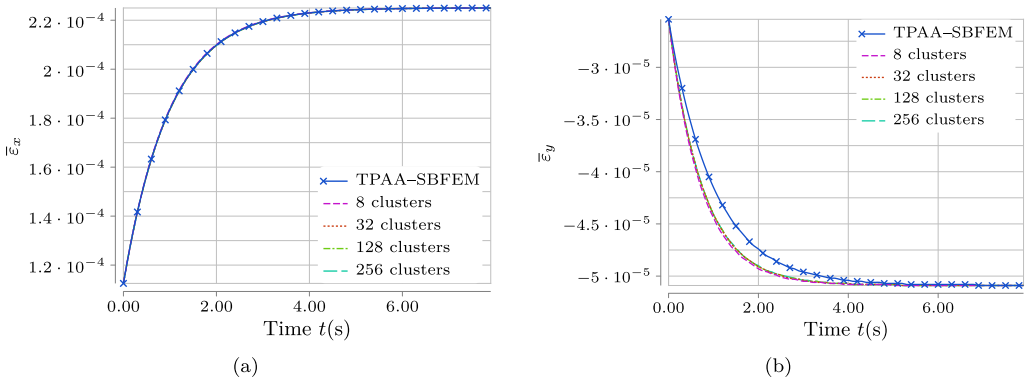

Fig. 9. Comparisons of time varying effective strains.

Table 8
A comparison of computational efficiency with respect to different step sizes.

Method	Step size	Proposed method				TPAA-SBFEM
		8 clusters	16 clusters	32 clusters	64 clusters	
CPU time	$\Delta t = 0.1$	8.8 s	9.3 s	9.4 s	9.5 s	87.3 s
	$\Delta t = 0.01$	9.3 s	9.5 s	9.7 s	10.0 s	731.3 s

Table 9
A comparison of effective parameters obtained with different number of clusters.

	$\overline{\mu}$	J_∞	J_1	τ_1	J_2	τ_2
Cluster = 8	0.230564268	0.0002246	−0.0001127	1.000	$7.994 * 10^{-7}$	10.00
Cluster = 32	0.230263761	0.0002252	−0.0001124	1.000	$-3.511 * 10^{-7}$	10.00
Cluster = 128	0.230218048	0.0002252	−0.0001125	1.000	$-3.084 * 10^{-7}$	10.00
Cluster = 256	0.230157321	0.0002252	−0.0001124	1.000	$-3.291 * 10^{-7}$	10.00
TPAA-SBFEM	0.226063572	0.0002251	−0.0001124	1.000	$-1.495 * 10^{-8}$	10.00

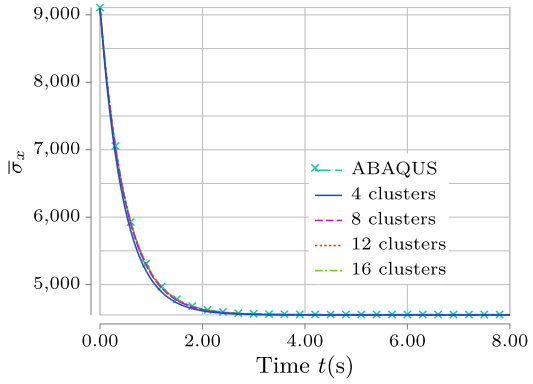

Fig. 10. Comparisons of time varying effective stress.

Table 10
The maximum relative deviation between the proposed method and ABAQUS.

	ABAQUS	4 clusters	8 clusters	12 clusters	16 clusters
Relative deviations	–	0.27%	0.046%	0.045%	0.028%

CRediT authorship contribution statement

Qiang Fu: Writing – original draft, Writing – review & editing. **Yiqian He:** Validation. **Xinglin Guo:** Validation. **Haitian Yang:** Validation, Conceptualization, Supervision.

Declaration of competing interest

The authors declare that they have no known competing financial interests or personal relationships that could have appeared to influence the work reported in this paper.

Acknowledgments

The research leading to this paper is funded by National Natural Science Foundation of China [11972109, 11572068, 11572077] and National Key Basic Research and Development Program of China [2015CB057804].

Appendix. Evaluation of effective creep compliance

In the case of constant stress boundary condition with $\widetilde{\sigma}$, the relationship between effective strain and stress is assumed to be

$$\overline{\varepsilon}(t) = \overline{J}(t) \cdot \overline{\sigma} \tag{A.1}$$

where $\overline{J}(t)$ refers to the effective creep compliance.

In this paper, $\overline{J}(t)$ is specified by Prony series,

$$\overline{J}(t) = \overline{J}_\infty + \sum_{i=1}^{N} \overline{J}_i * e^{-t/\overline{\tau}_i} \tag{A.2}$$

All the coefficients in $\overline{J}(t)$ can be determined by solving an optimization problem defined by

$$min: \quad \phi = \sum_{n=0}^{K} \| \overline{J}(t_n) \cdot \widetilde{\sigma} - \overline{\varepsilon}(t_n) \|^2 \tag{A.3}$$

where $\overline{\varepsilon}(t_n)$ refers to $\overline{\varepsilon}(t)|_{t=t_n}$, and K stands for the number of sample points in the time domain.

References

[1] H. Sabar, M. Berveiller, V. Favier, S. Berbenni, A new class of micro-macro models for elastic-viscoplastic heterogeneous materials, Int. J. Solids Struct. 39 (12) (2002) 3257–3276.
[2] J. Mandel, Cours de mécanique des milieux continus, 1966.
[3] N. Lahellec, P. Suquet, Effective behavior of linear viscoelastic composites: A time-integration approach, Int. J. Solids Struct. 44 (2) (2007) 507–529.
[4] T. Tian, S.D. Felicelli, Effective creep response and uniaxial tension behavior of linear visco-elastic polymer composites, 2015.
[5] J.F. Barthélémy, A. Giraud, F. Lavergne, J. Sanahuja, The Eshelby inclusion problem in ageing linear viscoelasticity, Int. J. Solids Struct. 97–98 (2016) 530–542.
[6] S.-T. Nguyen, Effect of pore shape on the effective behavior of viscoelastic porous media, Int. J. Solids Struct. 125 (2017) 161–171.
[7] D. Allen, C. Yoon, Homogenization techniques for thermoviscoelastic solids containing cracks, Int. J. Solids Struct. 35 (31–32) (1998) 4035–4053, http://dx.doi.org/10.1016/s0020-7683(97)00299-0.
[8] P.W. Chung, K.K. Tamma, R.R. Namburu, A micro/macro homogenization approach for viscoelastic creep analysis with dissipative correctors for heterogeneous woven-fabric layered media, Compos. Sci. Technol. 60 (12) (2000) 2233–2253.
[9] M.E.B. Seck, M. Garajeu, R. Masson, Effective nonlinear viscoelastic behaviour of particulate composites under isotropic loading, Eur. J. Mech. A (2017) URL https://hal.archives-ouvertes.fr/hal-01653258.
[10] J. Noh, J. Whitcomb, Efficient techniques for predicting viscoelastic behavior of sublaminates, Composites B 34 (8) (2003) 727–736, http://dx.doi.org/10.1016/s1359-8368(03)00082-9.
[11] A. Muliana, J.S. Kim, A concurrent micromechanical model for predicting nonlinear viscoelastic responses of composites reinforced with solid spherical particles, Int. J. Solids Struct. 44 (21) (2007) 6891–6913.
[12] J. Sanahuja, Effective behaviour of ageing linear viscoelastic composites: Homogenization approach, Int. J. Solids Struct. 50 (19) (2013) 2846–2856.
[13] J.D. Eshelby, The determination of the elastic field of an ellipsoidal inclusion, and related problems, Proc. R. Soc. Lond. Ser. A Math. Phys. Eng. Sci. 241 (1226) (1957) 376–396.
[14] R. Hill, A self-consistent mechanics of composite materials, J. Mech. Phys. Solids 13 (4) (1965) 213–222, http://dx.doi.org/10.1016/0022-5096(65)90010-4.
[15] R.M. Christensen, K.H. Lo, Solutions for effective shear properties in three phase sphere and cylinder models, J. Mech. Phys. Solids 27 (4) (1979) 315–330.
[16] T. Mori, K. Tanaka, Average stress in matrix and average elastic energy of materials with misfitting inclusions, Acta Metall. 21 (5) (1973) 571–574.
[17] Y. Benveniste, A new approach to the application of Mori-Tanaka's theory in composite materials, Mech. Mater. 6 (2) (1987) 147–157.

[18] R.M. Christensen, Viscoelastic properties of heterogeneous media, J. Mech. Phys. Solids 17 (1) (1969) 23–41.

[19] R.N. Yancey, M.J. Pindera, Micromechanical analysis of the creep response of unidirectional composites, J. Eng. Mater. Technol. 112 (2) (1990) 157–163.

[20] Y.M. Wang, G.J. Weng, The influence of inclusion shape on the overall viscoelastic behavior of composites, J. Appl. Mech. 59 (3) (1992) 510–518.

[21] M. Megnis, J. Varna, D.H. Allen, A. Holmberg, Micromechanical modeling of viscoelastic response of GMT composite, J. Compos. Mater. 35 (10) (2001) 849–882.

[22] K. Li, X.L. Gao, A.K. Roy, Micromechanical modeling of viscoelastic properties of carbon nanotube-reinforced polymer composites, Mech. Compos. Mater. Struct. 13 (4) (2006) 317–328.

[23] H. Hoang-Duc, G. Bonnet, A series solution for the effective properties of incompressible viscoelastic media, Int. J. Solids Struct. 51 (2) (2014) 381–391.

[24] F. Lavergne, K. Sab, J. Sanahuja, M. Bornert, C. Toulemonde, Homogenization schemes for aging linear viscoelastic matrix-inclusion composite materials with elongated inclusions, Int. J. Solids Struct. 80 (2016) 545–560.

[25] S.T. Nguyen, M.B. Vu, M.N. Vu, Q.D. To, A homogenization approach for the effective drained viscoelastic properties of 2D porous media and an application for cortical bone, J. Mech. Behav. Biomed. Mater. 78 (2017) 134–142.

[26] T. Honorio, B. Bary, J. Sanahuja, F. Benboudjema, Effective properties of n-coated composite spheres assemblage in an ageing linear viscoelastic framework, Int. J. Solids Struct. 124 (2017) 1–13, http://dx.doi.org/10.1016/j.ijsolstr.2017.04.028, URL http://www.sciencedirect.com/science/article/pii/S0020768317301853.

[27] N. Ma, S. Liu, Study on the thermal stress relaxation and constitutive equations of viscoelastic composite materials, Part II: Numerical simulation, Fuhe Cailiao Xuebao/Acta Mater. Compos. Sin. 22 (1) (2005) 158–163.

[28] G. Haasemann, V. Ulbricht, Numerical evaluation of the viscoelastic and viscoplastic behavior of composites, Tech. Mech. 30 (1–3) (2010) 122–135.

[29] G. Cheng, X. Li, Y. Nie, H. Li, FEM-Cluster based reduction method for efficient numerical prediction of effective properties of heterogeneous material in nonlinear range, Comput. Methods Appl. Mech. Eng. 348 (2019) 157–184, http://dx.doi.org/10.1016/j.cma.2019.01.019.

[30] A. Bensoussan, J.-L. Lions, G. Papanicolaou, T.K. Caughey, Asymptotic analysis of periodic structures, J. Appl. Mech. 46 (2) (1979) 477, http://dx.doi.org/10.1115/1.3424588.

[31] Non-Homogeneous Media and Vibration Theory, Springer Berlin Heidelberg, 1980, http://dx.doi.org/10.1007/3-540-10000-8.

[32] Y.M. Yi, S.M. Park, S.K. Youn, Asymptotic homogenization of viscoelastic composites with periodic microstructures, Int. J. Solids Struct. 35 (17) (1998) 2039–2055.

[33] W.H. Liu, X.M. Zhang, C.Y. Zhang, Asymptotic homogenization of viscoelastic composites, Eng. Mech. 22 (6) (2005) 63–68.

[34] W.H. Liu, X.M. Zhang, C.Y. Zhang, Application of homogenization theory to viscoelastic multilayered composites, Chin. J. Comput. Mech. 22 (6) (2005) 722–727.

[35] S. Liu, N. Ma, Study on the thermal stress relaxation and constitutive equations of viscoelastic composite materials, part I:general theory, Acta Mater. Compos. Sin. 22 (1) (2005) 152–157.

[36] T. Tian, S.D. Felicelli, Computational evaluation of effective stress relaxation behavior of polymer composites, Int. J. Eng. Sci. 90 (2015) 76–85.

[37] P.W. Chung, K.K. Tamma, R.R. Namburu, A finite element thermo-viscoelastic creep approach for heterogeneous structures with dissipative correctors, Finite Elem. Anal. Des. 36 (3–4) (2000) 279–313, http://dx.doi.org/10.1016/s0168-874x(00)00037-8.

[38] Z. Ruo-Jing, H.E. Wei, X.U. Zhen-Yu, Viscoelastic parameters of fiber reinforced plastics, J. Tongji Univ. (2002).

[39] X. Zhenyu, The viscoelastic response of fiber-reinforced composite material, Chin. J. Appl. Mech. (2003).

[40] W. Yu, T. Tang, Variational asymptotic method for unit cell homogenization of periodically heterogeneous materials, Int. J. Solids Struct. 44 (11–12) (2007) 3738–3755.

[41] A.A. Gusev, Time domain finite element estimates of dynamic stiffness of viscoelastic composites with stiff spherical inclusions, Int. J. Solids Struct. 88–89 (2016) 79–87, http://dx.doi.org/10.1016/j.ijsolstr.2016.03.021.

[42] T. Kanit, S. Forest, I. Galliet, V. Mounoury, D. Jeulin, Determination of the size of the representative volume element for random composites: statistical and numerical approach, Int. J. Solids Struct. 40 (13–14) (2003) 3647–3679, http://dx.doi.org/10.1016/s0020-7683(03)00143-4.

[43] H. Zhang, L. Li, Modeling inclusion problems in viscoelastic materials with the extended finite element method, Finite Elem. Anal. Des. 45 (10) (2009) 721–729, http://dx.doi.org/10.1016/j.finel.2009.06.006.

[44] S. Ghosh, K. Lee, S. Moorthy, Two scale analysis of heterogeneous elastic-plastic materials with asymptotic homogenization and Voronoi cell finite element model, Comput. Methods Appl. Mech. Eng. 132 (1–2) (1996) 63–116, http://dx.doi.org/10.1016/0045-7825(95)00974-4.

[45] Y. He, J. Guo, H. Yang, Q. Fu, Numerical prediction of effective properties for heterogeneous viscoelastic materials via a temporally recursive adaptive quadtree SBFEM, Finite Elem. Anal. Des. 177 (2020) 103426, http://dx.doi.org/10.1016/j.finel.2020.103426.

[46] Z. Liu, M. Bessa, W.K. Liu, Self-consistent clustering analysis: An efficient multi-scale scheme for inelastic heterogeneous materials, Comput. Methods Appl. Mech. Eng. 306 (2016) 319–341, http://dx.doi.org/10.1016/j.cma.2016.04.004.

[47] Transformation field analysis of inelastic composite materials, Proc. R. Soc. Lond. Ser. A Math. Phys. Eng. Sci. 437 (1900) (1992) 311–327, http://dx.doi.org/10.1098/rspa.1992.0063.

[48] J. Michel, P. Suquet, Nonuniform transformation field analysis, Int. J. Solids Struct. 40 (25) (2003) 6937–6955, http://dx.doi.org/10.1016/s0020-7683(03)00346-9.

[49] S. Roussette, J. Michel, P. Suquet, Nonuniform transformation field analysis of elastic–viscoplastic composites, Compos. Sci. Technol. 69 (1) (2009) 22–27, http://dx.doi.org/10.1016/j.compscitech.2007.10.032.

[50] K. Karhunen, Zur spektral theorie stochastischer prozesse, Ann. Acad. Sci. Fenn. (1946).

[51] M. Loeve, Probability Theory. Foundations. Random Sequences, Van Nostrand, 1955.

[52] I. Jolliffe, N.A. Jolliffe, Principal Component Analysis, second ed., in: Springer Series in Statistics, 2002.

[53] G. Berkooz, P. Holmes, J.L. Lumley, The proper orthogonal decomposition in the analysis of turbulent flows, Annu. Rev. Fluid Mech. 25 (1) (1993) 539–575, http://dx.doi.org/10.1146/annurev.fl.25.010193.002543.

[54] J. Yvonnet, Q.C. He, The reduced model multiscale method (R3M) for the non-linear homogenization of hyperelastic media at finite strains, J. Comput. Phys. 223 (1) (2007) 341–368, http://dx.doi.org/10.1016/j.jcp.2006.09.019.

[55] O. Goury, D. Amsallem, S.P.A. Bordas, W.K. Liu, P. Kerfriden, Automatised selection of load paths to construct reduced-order models in computational damage micromechanics: from dissipation-driven random selection to Bayesian optimization, Comput. Mech. 58 (2) (2016) 213–234, http://dx.doi.org/10.1007/s00466-016-1290-2.

[56] P. Ladevèze, Nonlinear computational structural mechanics: New approaches and non-incremental methods of calculation, in: Nonlinear Computation Structural Mechanics—New Approaches and Non-Incremental Methods of Calculation, 1999.

[57] A. Ammar, B. Mokdad, F. Chinesta, R. Keunings, A new family of solvers for some classes of multidimensional partial differential equations encountered in kinetic theory modeling of complex fluids, J. Non-Newton. Fluid Mech. 139 (3) (2006) 153–176, http://dx.doi.org/10.1016/j.jnnfm.2006.07.007.

[58] P. Ladevèze, J.-C. Passieux, D. Néron, The LATIN multiscale computational method and the proper generalized decomposition, Comput. Methods Appl. Mech. Eng. 199 (21–22) (2010) 1287–1296, http://dx.doi.org/10.1016/j.cma.2009.06.023.

[59] F. Chinesta, A. Ammar, A. Leygue, R. Keunings, An overview of the proper generalized decomposition with applications in computational rheology, J. Non-Newton. Fluid Mech. 166 (11) (2011) 578–592, http://dx.doi.org/10.1016/j.jnnfm.2010.12.012.

[60] C. Ghnatios, F. Masson, A. Huerta, A. Leygue, E. Cueto, F. Chinesta, Proper generalized decomposition based dynamic data-driven control of thermal processes, Comput. Methods Appl. Mech. Eng. 213–216 (2012) 29–41, http://dx.doi.org/10.1016/j.cma.2011.11.018.

[61] D. Néron, P.-A. Boucard, N. Relun, Time-space PGD for the rapid solution of 3D nonlinear parametrized problems in the many-query context, Int. J. Numer. Methods Eng. 103 (4) (2015) 275–292, http://dx.doi.org/10.1002/nme.4893.

[62] Y. Nie, G. Cheng, X. Li, L. Xu, K. Li, Principle of cluster minimum complementary energy of FEM-cluster-based reduced order method: fast updating the interaction matrix and predicting effective nonlinear properties of heterogeneous material, Comput. Mech. (2019).

[63] Y. Nie, Z. Li, G. Cheng, Efficient prediction of the effective nonlinear properties of porous material by FEM-Cluster based Analysis (FCA), Comput. Methods Appl. Mech. Engrg. 383 (3) (2021) 113921.

[64] S. Tang, L. Zhang, W.K. Liu, From virtual clustering analysis to self-consistent clustering analysis: a mathematical study, Comput. Mech. 62 (6) (2018) 1443–1460, http://dx.doi.org/10.1007/s00466-018-1573-x.

[65] R.M. Christensen, L.B. Freund, Theory of Viscoelasticity, Academic Press, 1982, p. 720.

[66] T. Mura, Micromechanics of Defects in Solids, 1987.

[67] L. Zhang, H. Yang, A 2-D numerical analysis for the structure composed by viscoelastic functionally graded materials using a temporally piecewise adaptive algorithm, Appl. Math. Model. 81 (2020) 441–456, http://dx.doi.org/10.1016/j.apm.2020.01.015.

[68] Y. Yu, Y. He, H. Yang, An adaptive recursive SBFE algorithm for the dynamic analysis of Viscoelastic problems, Eng. Anal. Bound. Elem. 128 (2021) 171–187, http://dx.doi.org/10.1016/j.enganabound.2021.04.002.

[69] S. Lloyd, Least squares quantization in PCM, IEEE Trans. Inf. Theory 28 (2) (1982) 129–137, http://dx.doi.org/10.1109/tit.1982.1056489.

[70] A. Saputra, H. Talebi, D. Tran, C. Birk, C. Song, Automatic image-based stress analysis by the scaled boundary finite element method, Int. J. Numer. Methods Eng. 109 (5) (2016) 697–738, http://dx.doi.org/10.1002/nme.5304.

[71] Y. He, J. Guo, H. Yang, Image-based numerical prediction for effective thermal conductivity of heterogeneous materials: A quadtree based scaled boundary finite element method, Int. J. Heat Mass Transf. 128 (2019) 335–343, http://dx.doi.org/10.1016/j.ijheatmasstransfer.2018.08.099.

[72] C. Nguyen, X. Zhuang, L. Chamoin, X. Zhao, H. Nguyen-Xuan, T. Rabczuk, Three-dimensional topology optimization of auxetic metamaterial using isogeometric analysis and model order reduction, Comput. Methods Appl. Mech. Eng. 371 (2020) 113306, http://dx.doi.org/10.1016/j.cma.2020.113306.